https://doi.org/10.1595/205651318X696729 *Johnson Matthey Technol. Rev.*, 2018, **62**, (2), 134–149

JOHNSON MATTHEY
TECHNOLOGY REVIEW
www.technology.matthey.com

Rechargeable Multi-Valent Metal-Air Batteries

A review of research and current challenges in secondary multivalent metal-oxygen batteries

By Laurence J. Hardwick*
Stephenson Institute for Renewable Energy, Department of Chemistry, The University of Liverpool, Peach Street, Liverpool, L69 7ZD, UK

Carlos Ponce de León#
Faculty of Engineering and the Environment, University of Southampton, Highfield, Southampton, SO17 1BJ, UK

Email: *hardwick@liverpool.ac.uk; #capla@soton.ac.uk

Rechargeable metal-oxygen cells could exceed the stored energy of today's most advanced lithium-ion cells. However challenges exist that must be overcome to bring this technology into practical application. These challenges include, among others, the recharge and cyclability efficiency, materials development and improvements in fundamental understanding of the electrochemistry and chemistry inside the cell. The common challenges for the anode, including corrosion, passivation and dendrite formation and those for the air cathode and the electrolyte are summarised in this review for cells based on magnesium, calcium, aluminium, silicon, zinc and iron.

1. Introduction

Unlike a conventional battery where the reagents are contained within the cell, metal-air batteries utilise dioxygen (O_2) from the atmosphere, and consequently can be thought of as a battery-fuel cell hybrid. Rechargeable metal-air batteries, hereafter referred to as metal-O_2 batteries, could play an increasingly important role as an energy storage technology in consumer electronics, electric vehicles, stationary storage and defence, because of their high specific energy (energy per unit weight) and energy density (energy per unit volume). A schematic representation of the rechargeable metal-O_2 cell is shown in **Figure 1**.

In general, for non-aqueous metal-O_2, on discharge, metal ions formed at the metallic anode are transported across the electrolyte and into the pores of the air cathode. O_2 from the atmosphere enters the cathode, and dissolves into the electrolyte within the pores. It is then reduced at the porous carbon electrode surface by electrons from the external circuit and combines with the metal ion (M^{n+}) from the electrolyte, leading to the formation of a solid metal oxide (M_xO_y) as the final discharge product. Remarkably the reaction is, to varying degrees, reversible. The metal oxide can be electrochemically oxidised, releasing oxygen gas, thus making this an energy storage device.

In aqueous metal-O_2, because the solubility of oxygen in water is low at atmospheric pressure (0.2 mM, at 25°C, 1 atm.) it is necessary to use oxygen in the gas phase not the liquid. Oxygen from the atmosphere diffuses into the porous carbon electrode, known as the gas diffusion electrode, by difference in pressure of oxygen between the outside and inside of the cell. Catalysts facilitate the reduction of oxygen to hydroxyl ions (in an alkaline electrolyte), with electrons generated from the oxidation of the metal anode. This may lead to the precipitation of a solid metal hydroxide ($M_x(OH)_y$) within the cell. The process is known as a three-phase reaction:

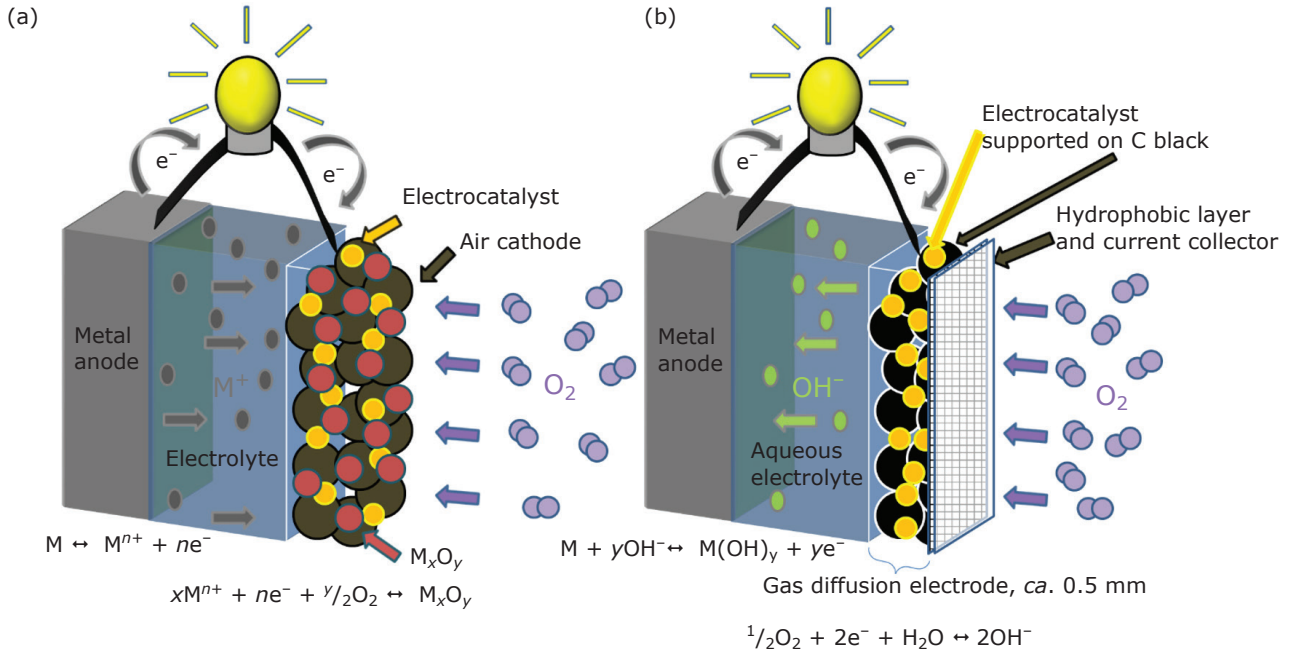

Fig. 1. Typical metal-O_2 batteries: (a) non-aqueous; and (b) aqueous

catalyst (solid), electrolyte (liquid) and oxygen (gas). A comparison of the phase boundaries of aqueous and non-aqueous metal-O_2 batteries is shown in **Figure 2**.

The reactions in non-aqueous and aqueous metal-O_2 cells are very different, and as such present differing challenges to enable their technological realisation, which will be discussed further within this review. Notably in non-aqueous electrolytes the oxygen reduction at the cathode results in the formation of a metal oxide precipitate within the porous cathode itself. However, in alkaline aqueous electrolyte the multivalent metal ion does not reach the cathode, as it will either be precipitated out by hydroxide ions, or form a negatively charged complex, in the vicinity of the anode (for example the zincate anion: $Zn(OH)_4^{2-}$), which will never reach the cathode.

Despite the recent major research activity into rechargeable Li-O_2 cells in particular (1–3), metal-O_2 batteries have in fact been under consideration from as early as 1868, with the first demonstration of a Zn-O_2 battery by Leclanché (4). Since this time some metal-O_2 technologies have moved from a purely academic interest to a commercial product, most notably the primary Zn-air battery.

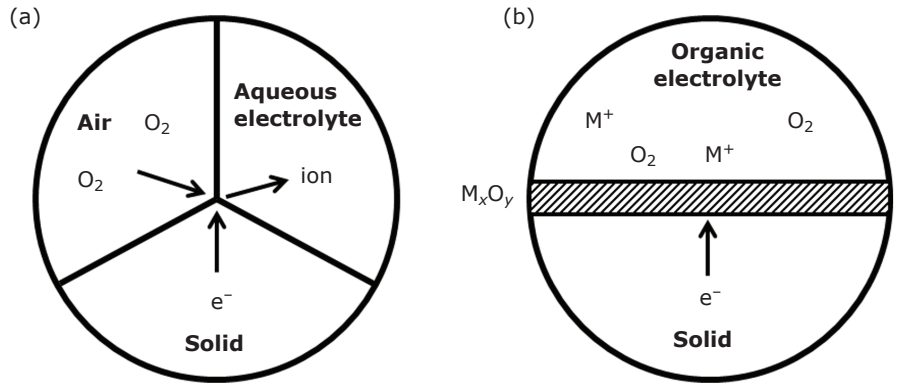

Fig. 2. Phase boundaries for (a) aqueous; and (b) non-aqueous metal-O_2 batteries

A substantial amount of work has been carried out on metal-O_2 batteries, but among the present challenges is the fundamental understanding and subsequent control of the electrochemistry and chemistry that takes place within metal-O_2 cells and the discovery of new materials that deliver the desired superior lifetime and performance (at a competitive cost). There are already a number of highly detailed reviews and articles on Li-O_2 (1, 5–8) and Na-O_2 (9, 10), as well as primary Zn-air systems (11). This review focuses on the recent work in rechargeable multivalent (+2, +3, +4) metal-O_2 cells, their operation, energy storage capability and the challenges they face in realisation of becoming a practical technology.

2. Theoretical Energy Storage

The theoretical specific energies (Wh kg^{-1}) (gravimetric energy densities) and energy densities (Wh dm^{-3}) (volumetric energy densities) for a range of metal-O_2 batteries are given in **Table I**, where they are compared with those for present day Li-ion cells. In the case of the non-aqueous Li-O_2 cell, a value of 11,586 Wh kg^{-1} is often quoted; however this is based on the mass of Li metal alone. All metal-O_2 cells gain mass (O_2) as they discharge, so the mass of O_2 should be included for all metal-O_2 systems.

The claim is often made that the increase in specific energy, in particular over conventional battery systems (Li-ion), is that the reactant dioxygen does not have to be carried within the cell. However, this is a misconception. The leap forward in theoretical specific energy on migrating from Li-ion to either aqueous or non-aqueous metal-O_2 (using Li-O_2 as the example) arises because Li_2O_2 in the cathode stores more Li, and hence charge, than say $LiCoO_2$ per unit mass and Li metal stores more charge per unit mass than a graphite (C_6Li) anode. Theoretical energy densities for aqueous metal-O_2 cells are also attractive. The theoretical energy density can be calculated by taking into account both the volume of the metallic anode in the charged state

Table I Data for Conventional Batteries Electrochemical Reactions for Common Metal-O_2 Couples that Form the Basis of Energy Storage Devices

Battery	Cell voltages, V	Theoretical specific energy, Wh kg^{-1}	Theoretical energy density, Wh dm^{-3} (active components in brackets)
Li-ion Today **$½C_6Li + Li_{0.5}CoO_2 = 3C + LiCoO_2$**	3.8	387	1015
Li metal/$LiCoO_2$ **$½Li + Li_{0.5}CoO_2 = LiCoO_2$**	3.9	534	2755
Li-O_2 (aq) **$2Li + ½O_2 + H_2O = 2LiOH$**	3.2	3582	2234 (Li + H_2O + LiOH)
Li-O_2 (non-aq) **$2Li + O_2 = Li_2O_2$** **$4Li + O_2 = 2Li_2O$**	2.959 2.913	3457 5226	3459 (Li + Li_2O_2) 3823 (Li + Li_2O)
Mg-O_2 (aq) **$Mg + ½O_2 + H_2O = Mg(OH)_2$**	3.11 1.2[a]	2859 1103	1671 (Mg + H_2O + $Mg(OH)_2$) *645* (Mg + H_2O + $Mg(OH)_2$)
Ca-O_2 (non-aq) **$Ca + O_2 = CaO_2$**	3.38	2514	2403 (Ca + CaO_2)
Al-O_2 (aq) **$2Al + ³⁄₂O_2 + 3H_2O = 2Al(OH)_3$**	2.71 1.2[a]	2794 1237	1160 (Al + H_2O + $Al(OH)_3$) *514* (Al + H_2O + $Al(OH)_3$)
Si-O_2 (ionic liquid) **$Si + O_2 = SiO_2$**	2.39 1.1[a]	4264 1962	2492 (Si + SiO_2) *1146* (Si + SiO_2)
Fe-O_2 (aq) **$Fe + ½O_2 + H_2O = Fe(OH)_2$**	1.28	764	715 (Fe + H_2O + $Fe(OH)_2$)
Zn-O_2 (aq) **$Zn + ½O_2 = ZnO$**	1.65	1086	6091 (ZnO) 2316 (Zn + ZnO)

[a]Experimentally recorded potentials on discharge of specific metal-O_2 cells – the theoretical energy storage of these systems are subsequently diminished (*in italic*). Theoretical energy density includes volume of all active components within the cell. Data taken from (1) or calculated directly from open source thermodynamic data.

and the volume of the discharge product (M_xO_y or $M_x(OH)_y$) formed from 100% utilisation of the anode. When H_2O is involved in the reaction, its volume requirement should also be considered, which lowers maximum energy densities of aqueous systems close to present day Li-ion.

The theoretical energy density is also greater for Li-O_2 than Li-ion but the gain is not as great as for specific energy. Certainly if the lithium metal anode would operate successfully in a Li-O_2 cell, then the positive energy storage benefit for the Li metal/$LiCoO_2$ cell would also be realised (**Table I**), as the energy density will be comparable to most metal-O_2 cells.

3. Common Challenges of Rechargeable Metal-Air Cells

3.1 Challenges for the Metallic Anode

Metallic anodes have been studied for many decades for numerous alternative battery systems other than metal-O_2, and the main challenges are well understood. The common issues with metallic anodes are corrosion, passivation and dendrite formation (**Figure 3**).

3.1.1 Corrosion

Corrosion of the metal anode is the major side reaction that limits the performance and shelf life of metal-O_2 cells. Most commonly corrosion results from the oxidation of the metal in an aqueous environment, either to a soluble metal ion or complex or to an insoluble oxide, hydroxide or other salt. In metal-O_2 batteries, the oxidising agent is commonly dioxygen, proton or water; hence the overall chemical change can occur *via* one or more of the reactions in Equations (i)–(iv):

$$M + {}^{n}/_{4}O_2 + {}^{n}/_{2}H_2O \rightarrow M^{n+} + nOH^- \quad (i)$$

$$M + {}^{n}/_{4}O_2 + nH^+ \rightarrow M^{n+} + {}^{n}/_{2}H_2O \quad (ii)$$

$$M + nH^+ \rightarrow M^{n+} + {}^{n}/_{2}H_2 \quad (iii)$$

$$M + nH_2O \rightarrow M^{n+} + {}^{n}/_{2}H_2 + nOH^- \quad (iv)$$

Oxidation by a proton can be avoided by the use of alkaline aqueous electrolytes (Equation (iv)).

An example of corrosion is given for the Fe-O_2 cell in Equations (v)–(ix). During spontaneous dissolution of iron, the electrode gradually becomes coated with a $Fe(OH)_2$ film as a result of the following corrosion reaction:

$$Fe \rightarrow Fe^{2+} + 2e^-$$
$$E_c = -0.44 \text{ V } \textit{vs}. \text{ SHE} \quad (v)$$

$$2H_2O + 2e^- \rightarrow 2OH^- + H_2$$
$$E_a = -0.83 \text{ V } \textit{vs}. \text{ SHE} \quad (vi)$$

Overall:

$$Fe + 2H_2O \rightarrow Fe(OH)_2 + H_2$$
$$E_{cell} = +0.39 \text{ V } \textit{vs}. \text{ SHE} \quad (vii)$$

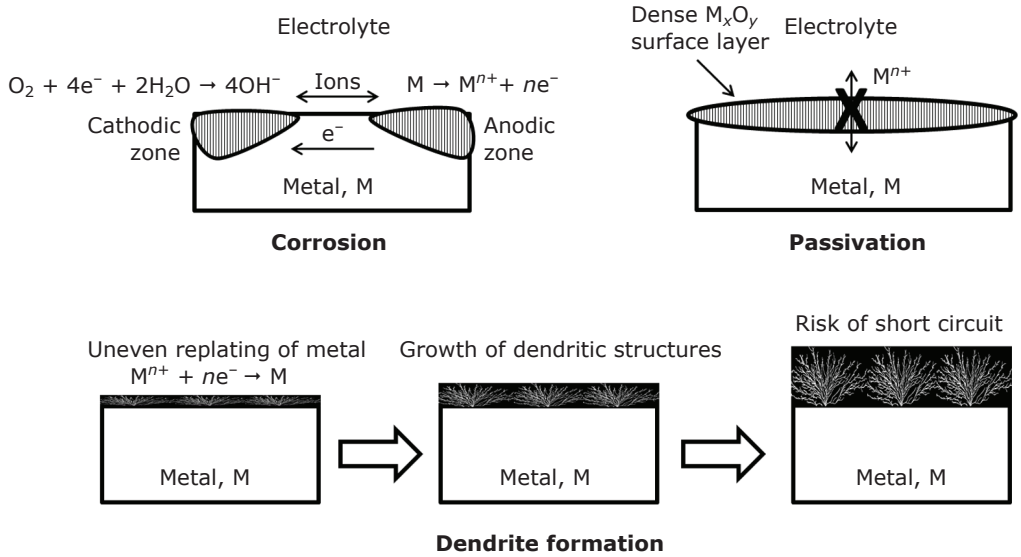

Fig. 3. Schematic showing corrosion, passivation and dendrite formation processes at metal anode

Remembering that for a corrosion reaction to be spontaneous:

$$E_{cell} = E_c - E_a > 0 \quad \text{(viii)}$$

$$\text{With } \Delta G = -nFE_{cell} = -75.5 \text{ kJ mol}^{-1} \quad \text{(ix)}$$

Therefore as $\Delta G < 0$, the reaction is thermodynamically favourable.

3.1.2 Passivation

Soluble species formed at the air cathode can migrate across to the anode where they can be reduced either chemically or electrochemically to form a non-conductive layer on the metal surface increasing the internal electrical resistance of the cell and preventing metal dissolution.

3.1.3 Dendritic Formation and Deformation

During the cycling of the metallic anode, the metal ion will not necessarily be plated where it has been stripped. As a consequence the metal electrode will start to change shape; its surface will roughen, producing an electrode with an uneven thickness. The restructuring of the metal will lead to the production of zones in the metal anode, which become less active, resulting in loss of performance. After repeated stripping and plating cycles, shedding of active material occurs leading to an irreversible loss of capacity. In worse cases the roughened surface results in dendritic growth of the metal which can eventually penetrate the cells' glass fibre separator and then form a short circuit with the air cathode. In aqueous systems this will result in the end of life of the cell and it will need to be replaced. In non-aqueous cells the result can be more catastrophic with the short-circuit leading to thermal runaway.

3.2 Challenges for the Air Cathode

The challenges for the air cathodes for both non-aqueous and aqueous metal-O_2 cells are shown in **Figure 4**. For non-aqueous systems a typical air cathode is comprised of a high surface area carbon mixed with a polymeric binder. The porous carbon air cathode is required to ensure a large electrolyte/electrode surface area and accommodate the insoluble discharge product (M_xO_y), as well as to facilitate oxygen diffusion to the reaction site through the cathode film. In addition, the porous carbon network must provide enough conductivity to deliver electrons to the reaction site efficiently with low overall impedance. High surface areas imply small pores that could become blocked by solid metal oxides, such as CaO_2, so a compromise is necessary between high active surface area and adequate pore size. For practical metal-O_2 cells, an exterior O_2 permeable membrane may be required to prevent the ingress of water and carbon dioxide, whilst still allowing the free passage of oxygen. In general the porous structure of the air cathode is not optimised for gas evolution. The mechanical pressures, which the carbon structure is subjected to as a result of the evolution of dioxygen produced trying to escape the electrode, will cause mechanical breakdown of the electrode, in addition to the high positive potential of oxygen evolution that leads to carbon corrosion.

In aqueous metal-O_2 air cathodes, a homogenous distribution of a nano-sized catalyst is required to maximise the performance by increasing the round-trip efficiency by lowering the voltage gap between charge and discharge processes (12). The structure of the air cathode is critical in order to maximise power capability. Nonetheless, the risk of mechanical degradation of the air cathode *via* O_2 evolution will increase at higher current densities. In aqueous systems gas diffusion electrodes are employed in which the gas is carried in hydrophobic channels then dissolves in the electrolyte within hydrophilic channels that are in very close proximity. In this way the O_2 is transported mainly in the gas phase, rather than the much slower diffusion in the liquid. Assuming a suitable gas diffusion electrode that ensures facile O_2 transport can be constructed, then a high electrode surface area is necessary. The proper optimisation of the air cathode should lessen the risk of electrode flooding from the electrolyte which would lead to a reduction in oxygen accessibility. A further challenge is to prevent the ingress of CO_2 which will lead to carbonate formation within the air cathode through reaction with the alkaline electrolyte.

3.3 Electrolytes for Metal-O_2 Batteries

Understanding, controlling and hence eliminating side reactions in metal-O_2 cells is a significant undertaking. The electrolyte must be stable to O_2 and its reduced species, as well as compounds that form on discharge; it must exhibit sufficient M^+ conductivity, O_2 solubility and diffusion to ensure satisfactory rate capability, as well as being able to wet the electrode.

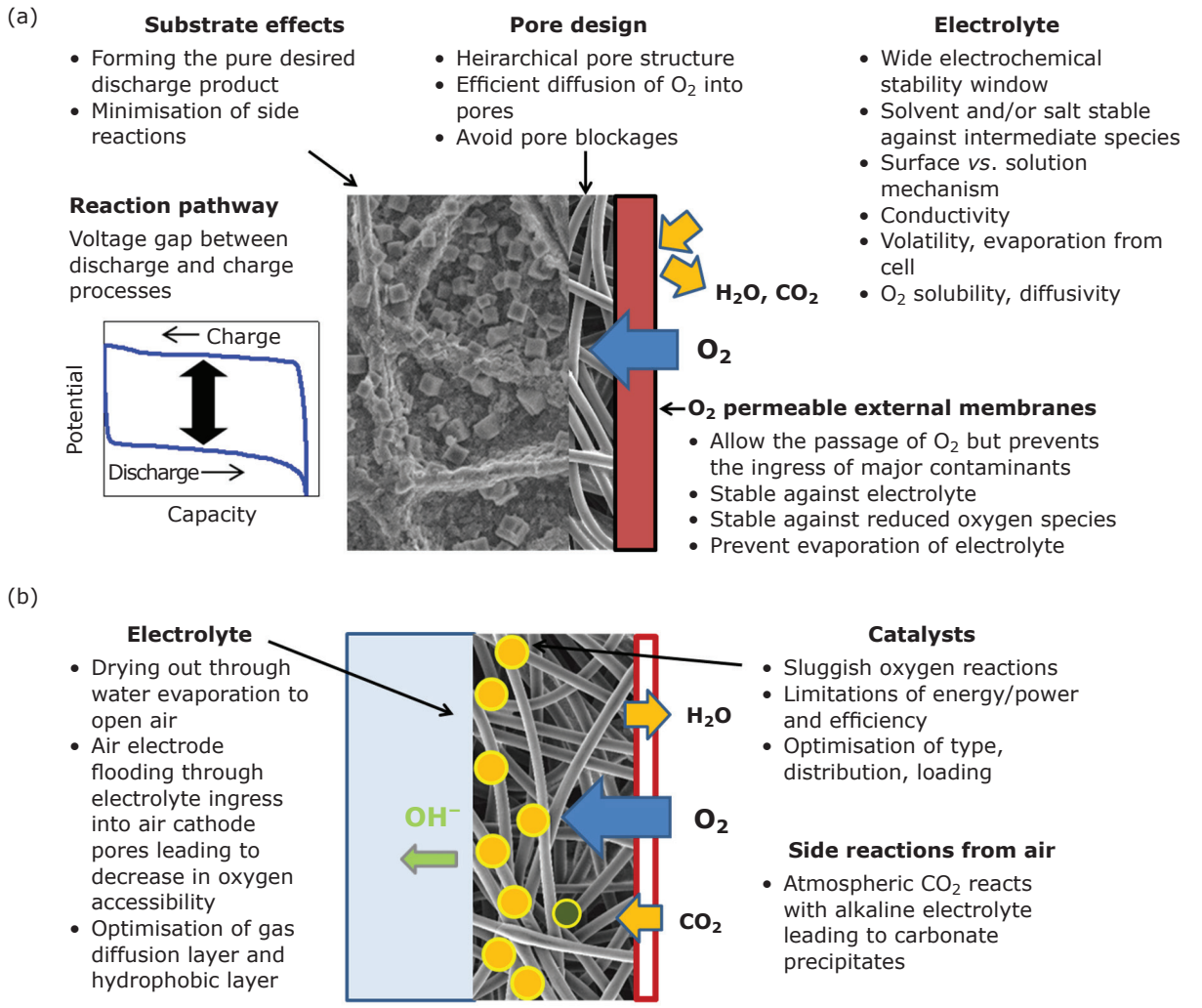

Fig. 4. Challenges facing: (a) the non-aqueous; and (b) the aqueous air cathode

The characteristics which a suitable metal-O_2 cell electrolyte must fulfil are listed below:

- resistive to nucleophilic attack from superoxide intermediates
- able to dissolve the electrolyte salt to sufficient concentration. In other words it should have a high dielectric constant (ε)
- high ionic conductivity (>1 mS cm^{-1}) in order to minimise internal resistance
- for liquid electrolytes, it should have low viscosity η, to facilitate mass transport
- high O_2 solubility and diffusivity
- stable in a wide electrochemical potential window
- good thermal and chemical stability
- compatibility with other cell components
- low cost, low toxicity and low flammability.

Developing stable electrolytes that fulfil most, if not all, of the above criteria remains one of the major research challenges in this field.

4. Alkaline-Earth Metal-O_2

4.1 Magnesium-O_2

Present Mg-O_2 research is limited and recent studies have focused on non-aqueous systems, magnesium alloys, suitable stable electrolytes and bifunctional electrocatalysts for oxygen reduction (13–18). A recent review article summarises the research to date (19).

For the aqueous based system the predicted cell voltage, according to Equations (x)–(xii), is 3.11 V, corresponding to a specific energy of 2859 Wh kg^{-1}:

Anode:

$$Mg \rightarrow Mg^{2+} + 2e^{-}$$
$$E_a = -2.7 \text{ V } \textit{vs.} \text{ SHE} \quad \text{(x)}$$

Cathode:

$$O_2 + 4e^{-} + 2H_2O \rightarrow 4OH^{-}$$
$$E_c = 0.401 \text{ V } \textit{vs.} \text{ SHE} \quad \text{(xi)}$$

Total:

$$2Mg + O_2 + 2H_2O \rightarrow 2Mg(OH)_2$$
$$E_{cell} = 3.11 \quad \text{(xii)}$$

As a primary battery, in aqueous solutions, Mg-O_2 suffers from high polarisation resulting in a practical cell voltage of 1.2 V. Despite the advantages of magnesium being abundant and a very active lightweight metal with relatively low toxicity, the cell has low coulombic efficiency due to the slow kinetics of the oxygen reduction and the high rates of magnesium corrosion. Magnesium can be mechanically replaced, but whilst operational suffers from irreversible polarisation and high self-discharge rates. In alkaline electrolytes, magnesium anodes passivate, but still show high corrosion rates, therefore aqueous Mg-O_2 systems use a sodium chloride solution. Even in this electrolyte, pure magnesium passivates over time and therefore some alloys such as Mg/Al/Zn have been proposed to mitigate against this (20).

4.2 Calcium-O_2

Until fairly recently there were no reports of reversible Ca metal stripping/plating in an organic solvent. The oxide passivation layer on Ca metal was found to be electronically and ionically insulating within a seminal study by Aurbach and coworkers (21). Recently Ponrouch *et al*. (22) demonstrated reversible Ca plating in an organic carbonate solvent with $Ca(BF_4)_2$ salt at 100°C and this has reignited research in calcium-based battery systems. In particular, electrochemical studies on the cathode side have followed (23, 24) that show some reversibility. However, finding an electrolyte that is good from reversible Ca plating/stripping and oxygen reduction/evolution reactions remains a major task. The challenges facing non-aqueous alkaline-earth metal-O_2 cells in particular are summarised in **Figure 5**.

In aqueous-based systems, calcium metal corrodes rapidly in water and Ca-O_2 batteries use an electrolyte containing 2:1 methanol:water ratio to decrease its reactivity. This electrolyte with 10% $(NH_4)_2SO_4$ plus 5% LiCl was used with a platinum air breathing electrode to produce a cell able to deliver 70 mA cm^{-2} at 1 V. Due to the limitations of the air cathode, a high temperature Ca-O_2 using a Ca-Si anode alloy in a molten salt with 29% mol of CaO-71 mol $CaCl_2$ stabilised with 5 wt% Zr-O at 850°C has been proposed (25). The charge-discharge processes are associated to the reversible formation of CaSi and $CaSi_2$, Equation (xiii):

$$2CaSi + {}^{1}/_{2}O_2 \rightleftarrows CaO + CaSi_2 \quad \text{(xiii)}$$

With an open circuit voltage of 2.28 V the battery operated for 52 h with a Faradaic efficiency of 95%. Other room temperature Ca-O_2 batteries use Ca or Ca alloy in acetonitrile or DMF and gas diffusion cathode (Co, Ni, Fe, and/or Mn or transition metal porphyrin or phthalocyanines). Cooper *et al*. (26) reported the passivation of Ca electrodes in 3 mol dm^{-3} NaOH but the addition of Cl^{-} produced stable electrodes. The open circuit voltage of the

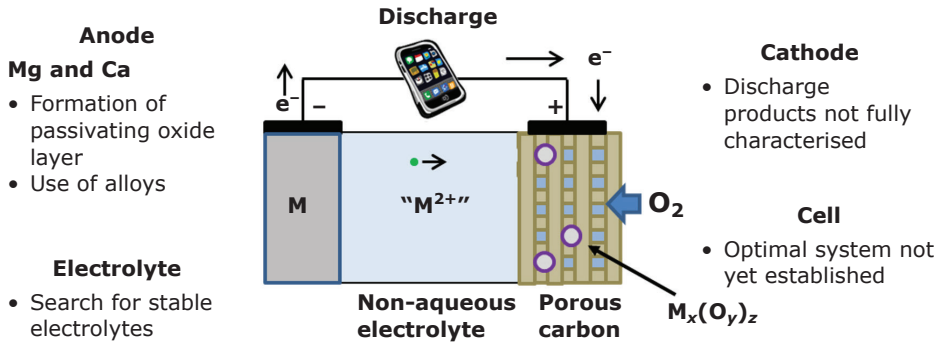

Fig. 5. Challenges for non-aqueous alkaline-earth metal-air batteries

cell was 3.1 V for <3 mol dm^{-3} OH^-, <0.1 mol dm^{-3} Cl^- and coulombic efficiency proportional to the concentration of Na approaching 100%. Based on these results the Ca-O_2 cell might operate at a thermodynamic efficiency of 35–40% for a cathode polarisation of 0.4 V and 100 mA cm^{-2} current density.

5. Aluminium-O_2

The ideal reactions for the Al-O_2 battery during discharge are Equations (xiv)–(xvi):

Anode:

$$Al + 4OH^- \rightarrow Al(OH)_4^- + 3e^- \qquad E_a = -2.31 \text{ V } \textit{vs.} \text{ SHE} \qquad \text{(xiv)}$$

Cathode:

$$O_2 + 2H_2O + 4e^- \rightarrow 4OH^- \qquad E_c = 0.401 \text{ V } \textit{vs.} \text{ SHE} \qquad \text{(xv)}$$

Total:

$$4Al + 3O_2 + 6H_2O \rightarrow 4Al(OH)_3 \qquad E_{cell} = 2.71 \text{ V} \qquad \text{(xvi)}$$

The theoretical specific energy is 2793 Wh kg^{-1} considering the product $Al(OH)_3$ and the cell voltage is 2.71 V. But in practice the available specific energy is lower as the operating voltage is usually around 1.1 V. The battery is a primary energy storage device since the electrodeposition of aluminium from alkaline solutions is not thermodynamically feasible due to its negative standard potential, leading to hydrogen evolution before any aluminium can be deposited. Mechanically recharging has been proposed by replacing the anode. Alternatively hydrogen evolution could be potentially removed by using ionic liquid electrolytes, where some studies show good plating reversibility (27).

The performance of an Al-O_2 battery is determined by the electrochemical and corrosion properties of the aluminium alloy electrode and the associated hydrogen gas evolution (28), Equations (xvii)–(xviii):

$$2H_2O + 2e^- \rightarrow 2OH^- + H_2 \qquad E = -0.83 \text{ V } \textit{vs.} \text{ SHE} \qquad \text{(xvii)}$$

$$2Al + 6H_2O \rightarrow 2Al(OH)_3 + 3H_2 \qquad \text{(xviii)}$$

Aluminium passivates in air or in aqueous solutions by formation of an oxide layer of several nanometre thicknesses which is detrimental to battery performance and restricts the ability to achieve the reversible potential causing delayed activation of the anode. The competing electrochemical processes on the Al surface are:

- formation and/or dissolution of an initial Al_2O_3 and subsequent $Al(OH)_3$ layer
- oxidation of Al to Al^{3+}
- formation of corrosion species – $Al(OH)_4^-$ and $Al(OH)_3$
- parasitic corrosion resulting in H_2 formation *via* water reduction.

Self-corrosion at open circuit prevents the storage of wet Al-O_2 cells and reduces their discharge efficiency. The corrosion and oxidation of Al in alkaline electrolytes depends on electrolyte properties, temperature and purity. Indeed one of the methods for suppressing parasitic corrosion whilst maintaining the electrode activity can be achieved by employing high purity aluminium (>99.999% purity) or by alloying the aluminium with minor amounts of indium, gallium, zinc, magnesium, tin or thallium. This of course will dramatically increase the cost of the anode (29).

It is essential to the battery performance that both the Al anode and air cathode can operate at a current density greater than 100 mA cm^{-2}. With a neutral brine electrolyte, the Al(III) is largely formed as a solid oxide and/or hydroxide and the performance of the battery depends critically on the form of this precipitate; it must not form a passivating film on the aluminium surface nor inhibit the air cathode. In addition, the Al material used as the negative electrode must be stable to corrosion during battery storage, i.e. the following chemical reactions (Equations (xix)–(xx)) should not occur at open circuit potential or during discharge:

$$4Al + 3O_2 + 6H_2O \rightarrow 4Al^{3+} + 12OH^- \qquad \text{(xix)}$$

$$2Al + 6H_2O \rightarrow 2Al^{3+} + 3H_2 + 6OH^- \qquad \text{(xx)}$$

The competing demands of stability to corrosion and rapid anodic dissolution makes difficult the identification of the appropriate aluminium alloy. Several alloys to suppress the hydrogen evolution and lower the self-corrosion of aluminium have been identified. Nevertheless the high cost of these high-purity aluminium alloys still restricts the commercialisation of Al-O_2 batteries and its use has been limited. **Figure 6** shows typical challenges and performance of an Al-O_2 battery, using gel electrolyte, bipolar electrodes and a flowing electrolyte (30).

Despite the operational barriers of the aluminium-air battery mentioned above, a number of studies dealing with hydrogen evolution and rechargeable

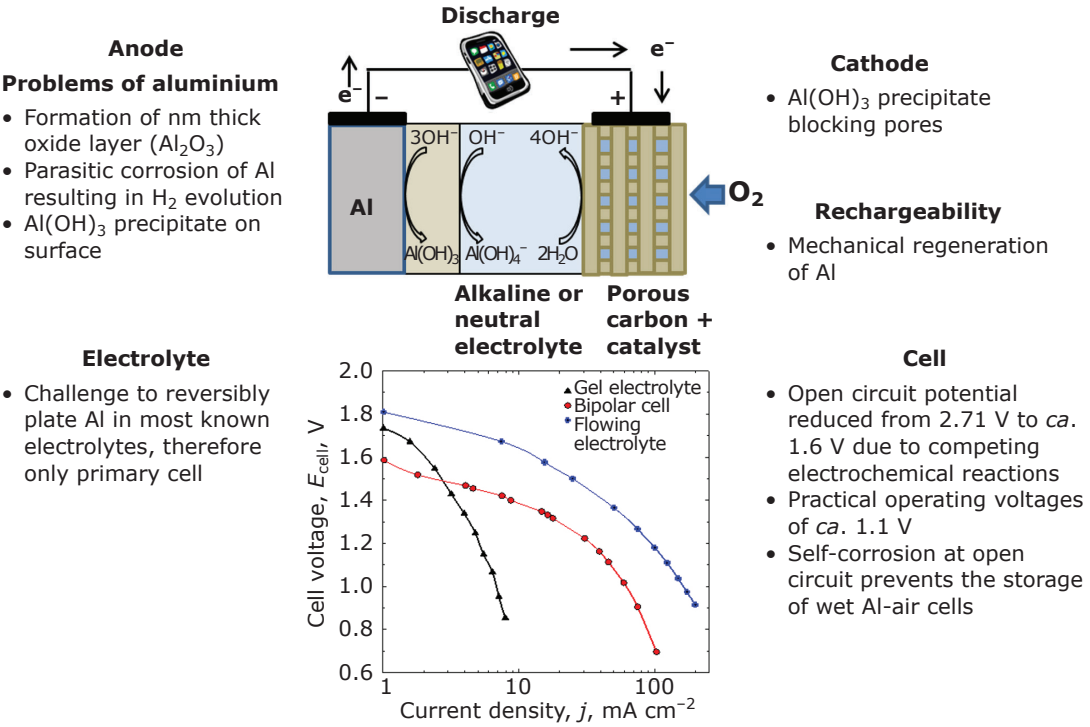

Fig. 6. Challenges for Al-air and typical performance curves for different primary Al-air configurations. Performance curve data provided by C. Ponce de Leon taken from (30) © Elsevier 2013

issues have been reported. Mori (31–33) for example, used ceramic barriers such as aluminium oxide or aluminium tungsten oxide between the aqueous electrolyte, the aluminium anode and the air cathode in order to suppress the accumulation of byproducts. However, the current densities remained low. The same author also suggested aluminium terephthalate metal-organic framework (MOF) for the air cathode and 1-ethyl-3-methylimidazolium chloride as an ionic liquid electrolyte in order to obtain more stability over repeated electrochemical reactions. Deyab used 1-allyl-3-methylimidazolium bis(trifluoromethylsulfonyl)imide ionic liquid to overcome the hydrogen evolution reaction (HER) (34). They suggested that 1.5×10^{-3} mol dm^{-3} added to a 4.0 mol dm^{-3} NaOH electrolyte resulted in an enhanced capacity from 1720 to 2554 mA h g^{-1}. Other attempts to use aluminium include a mechanical rechargeable Al-O_2 cell consisting of wedge anodes able to reach up to 1500 W h kg^{-1} energy density (35).

6. Silicon-O_2

A Si-O_2 battery was first reported by Ein-Eli and co-workers in 2009 (36) and theoretically the system has a specific energy of 4264 Wh kg^{-1}. It consisted of a doped silicon anode and carbon-based air cathode with the addition of MnO_2 as an oxygen reduction reaction (ORR) catalyst. The electrolyte employed within the cell was a room temperature hydrophilic ionic liquid, 1-ethyl-3-methylimidazolium oligofluorohydrogenate (EMI ($HF_{2.3}F$)), which is synthesised from EMI Cl and HF. The discharge of the cell results in the oxidation of silicon at the silicon wafer anode and in the reduction of atmospheric oxygen at the air cathode. The room temperature ionic liquid (RTIL) electrolyte anions participate in both electrode reactions and are therefore key in permitting the operation of the battery.

The reaction at the anode is Equation (xxi):

$$Si + 12(HF)_2F^- \rightarrow 8(HF)_3F^- + SiF_4 + 4e^- \quad \text{(xxi)}$$

And the reactions at the cathode are Equations (xxii)–(xxiii):

$$O_2 + 12(HF)_3F^- + 4e^- \rightarrow 2H_2O + 16(HF)_2F^- \quad \text{(xxii)}$$

$$SiF_4 + 2H_2O + 4(HF)_2F^- \rightarrow SiO_2 + 4(HF)_3F^- \quad \text{(xxiii)}$$

Leading to the overall reaction, Equation (xxiv):

$$Si + O_2 \rightarrow SiO_2 \quad \text{(xxiv)}$$

Cells tested show an open circuit potential of *ca*. 1.4 V rather than the theoretically predicted 2.89 V, the operating potential for this cell is in the 0.8–1.1 V region. The role of water in the Si-O_2 cell is central in the production of SiO_2 at the cathode, see Equation (xxiii). SiO_2 formation results in the reaction of H_2O with a fluororacidic anion [$(HF)_2F^-$] and with SiF_4. Indeed it has been demonstrated that this ionic liquid electrolyte with an addition of 15 vol% of water can increase cell capacity to 72.5 mAh cm^{-2} from 50 mAh cm^{-2} for water free electrolyte, at a current density of 0.3 mA cm^{-2}. The main challenges of Si-O_2 cells are illustrated within **Figure 7**.

Another variation of a Si-O_2 cell has also been considered in which the cell alternatively operates in an alkaline electrolyte (37–40) with specific capacity of 1206 mAh g^{-1} at 0.1 mA cm^{-2} with an operating voltage of 1 V being reported, Equations (xxv)–(xxvii).

Anode:

$$Si + 4\,OH^- \rightarrow Si(OH)_4 + 4e^- \quad E_a = -1.69 \text{ V } \textit{vs}. \text{ SHE} \quad \text{(xxv)}$$

Cathode:

$$O_2 + 2H_2O + 4e^- \rightarrow 4OH^- \quad E_c = 0.401 \text{ V } \textit{vs}. \text{ SHE} \quad \text{(xxvi)}$$

Leading to the overall reaction:

$$Si + O_2 + 2H_2O \rightarrow Si(OH)_4 \quad E_{cell} = 2.091 \text{ V} \quad \text{(xxvii)}$$

In alkaline electrolyte there is a side reaction that increases with respect to basicity, Equation (xxviii):

$$Si + 2OH^- + 2H_2O \rightarrow SiO_2(OH)_2^{2-} + 2H_2 \quad \text{(xxviii)}$$

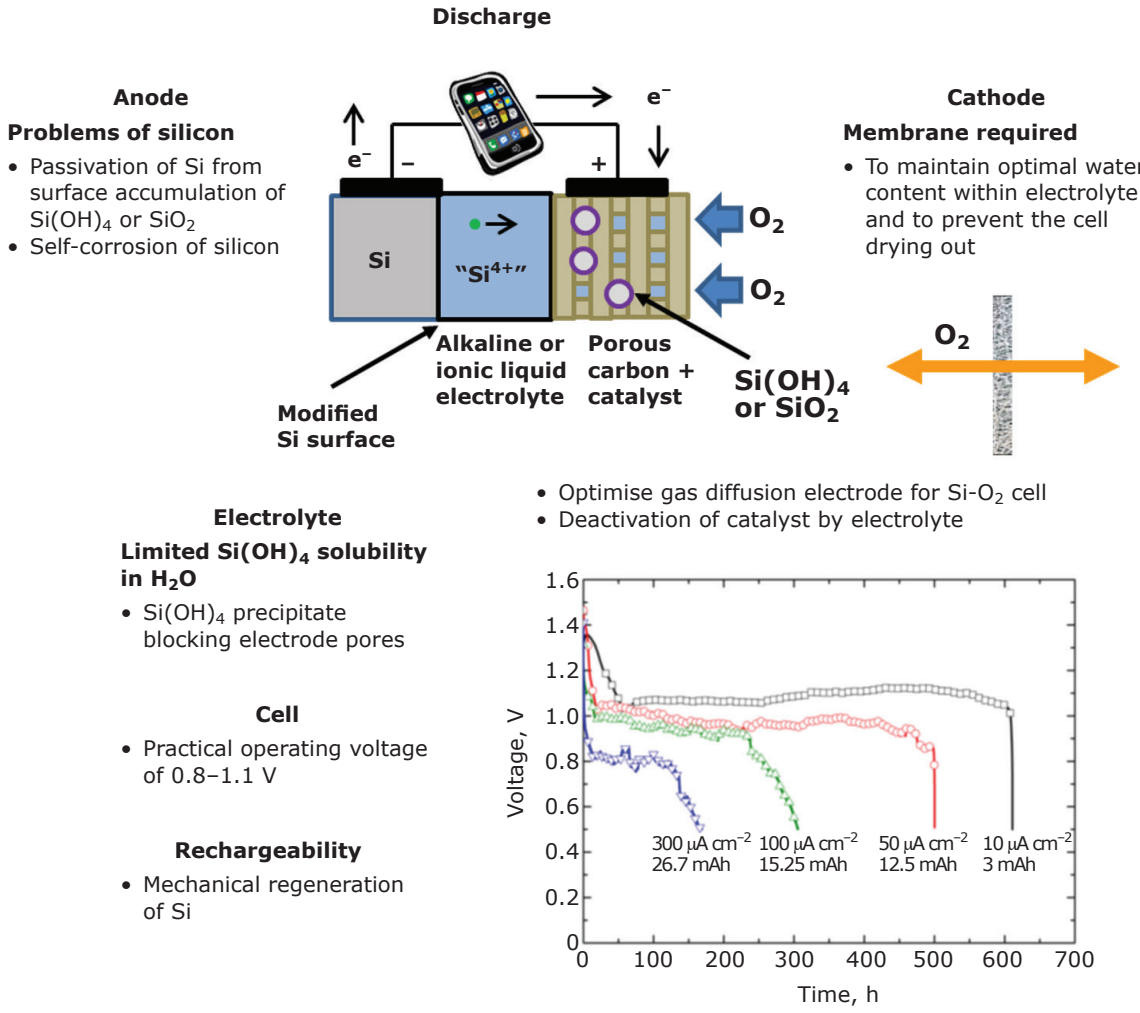

Fig. 7. Specific challenges facing the Si-O_2 battery and cell performance data using EMI·(HF)2.3F RTIL electrolyte at different constant current densities. Cycling data from figure reproduced from (41) © Elsevier 2010

7. Zinc-O_2

With a theoretical specific energy of 1086 Wh kg^{-1} the Zn-O_2 battery is one of the most studied metal-air systems offering low cost and relatively abundant materials (zinc, potassium hydroxide, carbon, manganese dioxide) (3, 42). The battery has an open circuit potential of 1.65 V in 6 M KOH and results from the elimination of the H_2 evolution reaction. This is due to the presence at the surface of the Zn metal electrode, of a thin ionically conducting, but electronically insulating layer of ZnO. Water is therefore excluded from the electrochemical interface, thus the effective stability range of the electrolyte is extended (Equations (xxix)–(xxxi)):

Anode:

$$Zn + 4OH^- \rightleftarrows Zn(OH)_4^{2-} + 2e^- \quad E_a = -1.199 \text{ V } vs. \text{ SHE} \qquad (xxix)$$

In solution:

$$Zn(OH)_4^{2-} \rightleftarrows ZnO + 2OH^- + H_2O \qquad (xxx)$$

Air cathode:

$$O_2 + 2H_2O + 4e^- \rightleftarrows 4HO^- \quad E_c = 0.401 \text{ V } vs. \text{ SHE} \qquad (xxxi)$$

Leading to the overall reaction, Equation (xxxii):

$$Zn + {}^1/_2O_2 \rightarrow ZnO \qquad E_{cell} = 1.6 \text{ V} \qquad (xxxii)$$

Zn is easily recyclable, thereby offering both a sustainable and low toxic energy storage device. The recycling process is as follows:

1. disassembly of the used Zn source (typically 80% Zn utilisation)
2. reaction of the Zn anode oxidation product (ZnO) with the electrolyte (KOH), Equation (xxxiii):

$$ZnO + 2KOH + H_2O \rightarrow K_2Zn(OH)_4 \qquad (xxxiii)$$

3. electrowinning of the zincate solution, Equation (xxxiv):

$$K_2Zn(OH)_4 \rightarrow Zn + 2KOH + H_2O + ½O_2 \qquad (xxxiv)$$

4. reassembly of the Zn source containing the electrowon Zn.

Millions of primary Zn-O_2 (Zn-air) batteries are sold annually for hearing aids and other medical devices. Commercially available cells can have very high specific energies and energy densities, up to 442 Wh kg^{-1} and 1672 Wh dm^{-3} respectively for the Duracell® Zn-air button cell. The primary Zn-air cell is a mature technology, which is not currently the case for rechargeable Zn-O_2 and offers a tantalising glimpse of its great promise, if the primary technology performance could be replicated in a secondary system. The principal disadvantage at present is the low cycle life of the cell when electrochemically recharged and a voltage gap (0.8 V under a load of 20 mA cm^{-2}) between discharge and charge processes.

Rechargeable Zn-O_2 suffers from two key drawbacks that do not affect the primary cell: the poor stability of the air cathode when used to charge the battery, and as in the earlier example of lithium metal, the formation of dendrites on the zinc anode leading to short circuits and shedding of zinc. Dendrite formation occurs as the Zn is replated from an electrolyte containing non-uniform zincate, $Zn(OH)_4^{2-}$ composition gradients and uneven ZnO at the surface. Gravitational demixing causes the concentration of zincate ions to increase at lower positions, resulting in slight differences in the conductivity of the electrolyte. Consequently there is a gradual redistribution of the zinc, so that the lower portions of the electrode become thicker as it is stripped and plated.

Rechargeable Zn-O_2 cells require zinc precipitation from the water-based electrolyte to be closely controlled. Challenges include dendrite formation, non-uniform zinc dissolution and limited solubility in electrolytes. Electrically reversing the reaction at a bifunctional air cathode, to liberate oxygen from discharge reaction products, is difficult; membranes tested to date have low overall efficiency. Charging voltage is much higher than discharge voltage, producing cycle energy efficiency as low as 50%. Providing charge and discharge functions by separate unifunctional cathodes increases cell size, weight and complexity.

A satisfactory electrically recharged system potentially offers low material cost and high specific energy. **Figure 8** summarises the main characteristics and challenges of a Zn-O_2 cell and shows the charge-discharge cycles of a cell with a hierarchical meso-macroporous lanthanum manganite ($LaMnO_3$) cathode at 25 mA cm^{-2} current density (43).

There has been a recent increase in interest in rechargeable Zn-air with a number of studies reported. In particular, Wu *et al*. (44) used a simple scalable procedure to manufacture porous bifunctional electrodes for the Zn-O_2 battery. The polyhedral carbon electrodes reported use a Zn-doped Co-based zeolitic imidazolate frameworks (ZnCo-ZIFs) precursor. The authors state that Zn doping produces small Co nanoparticles with high nitrogen content that enhances both the

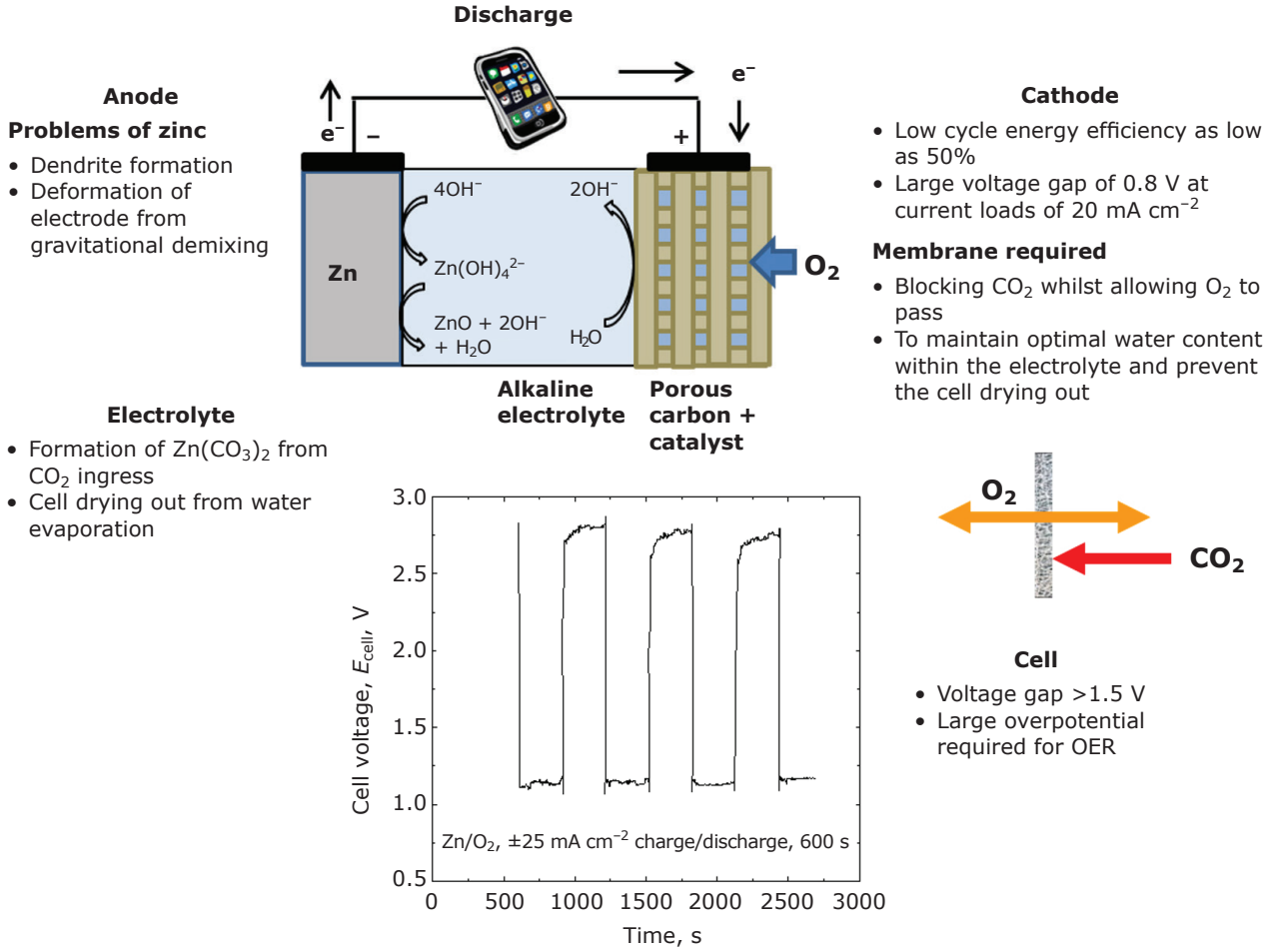

Fig. 8. Challenges and performance for rechargeable Zn-O_2. Charge, discharge cycle figure reproduced from performance curve data from (43) © Elsevier 2014

evolution and reduction of oxygen. The $ZnCoNC_x$ materials are highly graphitised with a porous polyhedral structure and large surface area. The authors reported a cell able to cycle up to 100 times at 7 mA cm^{-2} with only 10 mV difference between charge and discharge cycles. In another example, a composite material consisting of Co_3O_4 nanoparticles decorated with carbon nanofibers (CNFs) was used as a bifunctional electrode for the Zn-O_2 battery. Metal ion containing polymers were electrospun and carbonised to obtain the composite. The authors claimed that the electrode was able to yield four electrons during the reduction of oxygen, competing with commercial platinum electrodes, and that the prototype cell had an energy efficiency of 64% when charged/discharged at 1 mA cm^{-2} (45).

Recent reports have shown greatly improved cyclability under ambient conditions, with 100+ cycles being routinely presented. A number of catalysts have shown bifunctionality in order to overcome the sluggish kinetics of the oxygen evolution reaction (OER) and ORR with voltage hysteresis between 0.6–1 V at 10–20 mA cm^{-2}. These include transition metal hydroxysulfides (46), pyrolysised MOFs containing Zn and Co (47), Fe_3Mo_3C-supported IrMn Clusters (48), Ni_3FeN-supported Fe_3Pt intermetallic nanoalloys (49), $CoO_{0.87}S_{0.13}$ (50), carbon nitrides (51) and $Fe_{0.1}Ni_{0.9}Co_2O_4$ spinels (52).

8. Iron-O_2

Alkaline Fe-O_2 batteries were under intense industrial investigation during the 1970s and early 1980s, most notably by The Westinghouse Electric Corporation, USA, and the Swedish National Development Corporation, Sweden, for the application of an electric vehicle battery. The alkaline Fe-O_2 battery has a predicted open circuit cell voltage of about 1.28 V and a theoretical specific energy of 764 Wh kg^{-1} with the formation of $Fe(OH)_2$ (53).

Iron electrodes have been used for over 70 years in Ni/Fe batteries, and the notable advantages of this system are the availability, abundance and low cost

of iron. Iron electrodes are fabricated into sintered structures. The iron electrode is formed from high purity iron oxide powder in order to increase the overpotential for H_2 evolution. However, this adds significant cost to electrode fabrication. The Fe-O_2 battery substitutes the nickel electrode for an air breathing electrode which in theory could increase the specific energy by 100%.

The reactions at the anode are complex and still a matter of discussion and involve several intermediates. The reaction is also complicated by hydrogen evolution if the metallic iron corrodes to Fe(II), forming $Fe(OH)_2$, and the electrode gradually becomes coated with a film of $Fe(OH)_2$ as a result of the following reactions, Equations (xxxv)–(xxxviii):

$$Fe \rightarrow Fe^{2+} + 2e^- \quad E° = -0.447 \text{ V } \textit{vs}. \text{ SHE} \quad \text{(xxxv)}$$

$$Fe + 2OH^- \rightleftarrows Fe(OH)_2 + 2e^- \quad E° = -0.88 \text{ V } \textit{vs}. \text{ SHE} \quad \text{(xxxvi)}$$

$$2H_2O + 2e^- \rightarrow 2OH^- + H_2 \quad E° = -0.8277 \text{ V } \textit{vs}. \text{ SHE} \quad \text{(xxxvii)}$$

Total reaction:

$$Fe + 2H_2O \rightarrow Fe(OH)_2 + H_2 \quad \text{(xxxviii)}$$

If the HER, Equation (xxxviii), can be avoided the efficiency of the Fe-O_2 battery is greater. The formation of $Fe(OH)_2$ is followed by oxidation to Fe(III) forming magnetite, Fe_3O_4, Equation (xxxix):

$$3Fe(OH)_2 + 2OH^- \rightleftarrows Fe_3O_4 + 4H_2O + 2e^- \quad E_a = -0.76 \text{ V } \textit{vs}. \text{ SHE} \quad \text{(xxxix)}$$

The reaction at the cathode is the reduction of oxygen, Equation (xl):

$$½O_2 + H_2O + 2e^- \rightarrow 2OH^- \quad E_c = 0.401 \text{ V } \textit{vs}. \text{ SHE} \quad \text{(xl)}$$

The overall reaction where magnetite (as opposed to $Fe(OH)_2$) is the discharge product is Equation (xli):

$$3Fe + 2O_2 \rightarrow Fe_3O_4 \quad E_{cell} = 1.15 \text{ V} \quad \text{(xli)}$$

The manufacturing of the iron electrode involves additives such as bismuth and sulfur to minimise the corrosion of the iron electrode and the evolution of hydrogen in an attempt to favour Equations (xxxix) and (xl). The formation of magnetite Fe_3O_4 Equation (xli) leads to a lower cell voltage.

Problems that adversely affect the performance of the iron anode are spontaneous corrosion in the charged state (leading to a high rate of self-discharge), a low faradaic efficiency for the anodic dissolution reaction, poor low-temperature performance, and low charge acceptance at high ambient temperatures due to a parasitic HER. The challenges and performance of a Fe-O_2 cell are shown in **Figure 9**.

More recently a solid electrolyte based Fe-O_2 cell has been reported (56, 57). An oxide ion conductor is employed as the electrolyte and the cell operates at temperatures greater than 600°C. The solid oxide iron-air battery utilises the FeO-Fe phase equilibrium as a means of storing electrical-chemical energy *via* a series of H_2/H_2O-mediated reversible electrochemical-chemical looping reactions. The capacity and efficiency characteristics of this battery were found to be strongly dependent on the degree of iron utilisation: higher charge and energy storage capacity, but lower round-trip efficiency, can be produced at higher iron utilisation, and lower charge and energy storage capacity, but higher round trip efficiency, can be produced at lower iron utilisation.

A bifunctional carbon based air electrode containing 0.5 mg cm^{-2} loading of 30% palladium on carbon, reported by McKerracher *et al*. (58), was stable after 1000 charge/discharge cycles at 10 mA cm^{-2} in an Fe-O_2 alkaline battery. At higher current densities (20–80 mA cm^{-2}), the electrode showed better performance than some commercially produced platinum on carbon gas diffusion electrodes. The authors suggested that the better performance is due to the well-dispersed, nanoscale Pd particles. Figueredo-Rodríguez *et al*. (59) reported an Fe-O_2 battery with a specific energy of 764 W h kg^{-1} Fe and 453 W h kg^{-1} Fe energy density with a charge capacity of 814 mA h g^{-1} Fe when it was cycled at a current density of 10 mA cm^{-2}. The cell employed nanocomposite iron electrodes manufactured by iron oxide synthetised *via* a molten salt fusion method followed by mixing with a high surface area carbon by ball milling. The gas diffusion electrodes comprised three main parts bound together by hot pressing at 180°C and 250 kPa:

1. a gas diffusion layer composed of 80 wt% high surface area (*ca*. 64 m^2 g^{-1}) carbon mixed with 20 wt% polytetrafluoroethylene
2. a catalyst layer formed by 30 wt% Pd/C catalyst in a 5 wt% Nafion solution, and
3. an expanded nickel mesh current collector.

9. Conclusion

Modern society requires energy storage devices with much higher levels of energy storage than

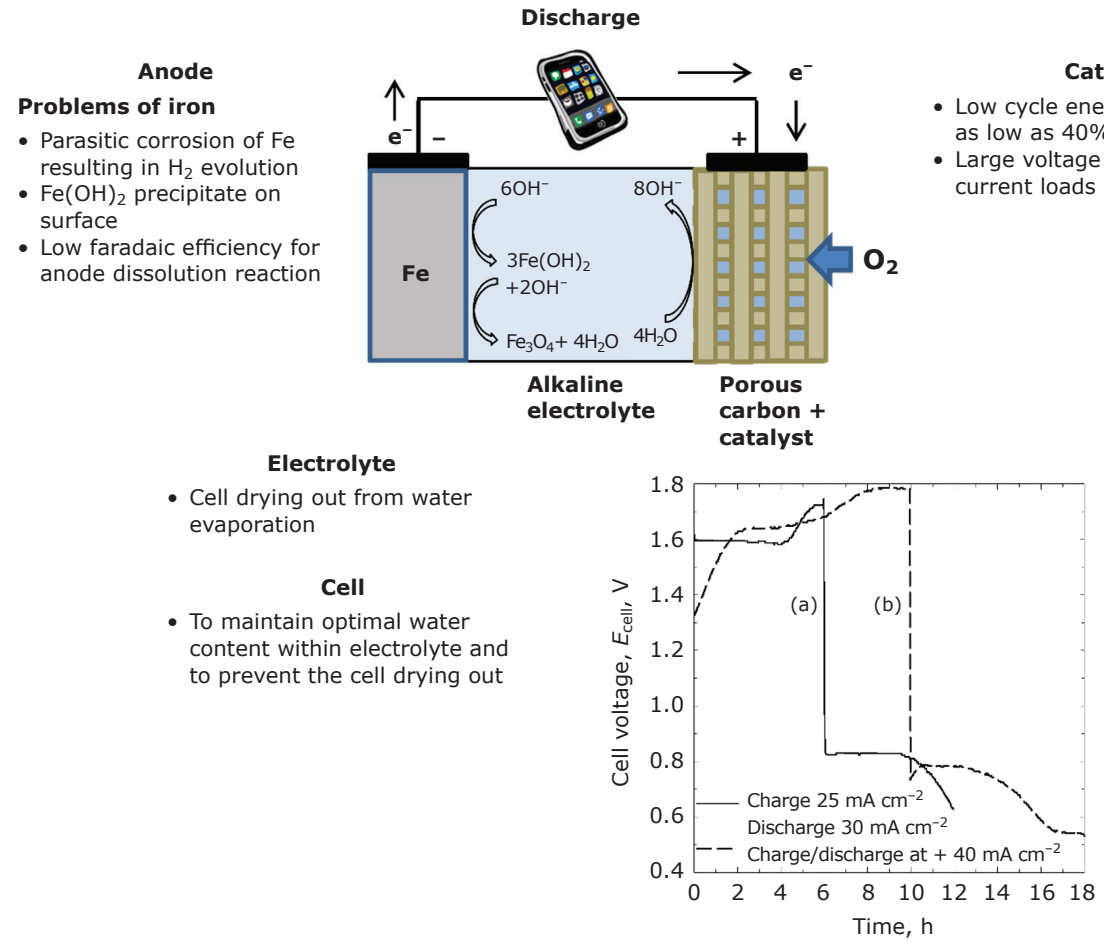

Fig. 9. Challenges and performance for Fe-O_2 and comparison of two charge-discharge cell potential curves for an Fe-O_2 battery: (a) 25 mA cm^{-2} charge discharged at 30 mA cm^{-2} of a prototype stack containing 190 air and 95 iron electrodes of 10 × 20 cm divided into 19 cells connected in series (54); (b) charge and discharge at 40 mA cm^{-2}, the cell contained air electrodes of 100 cm^2 area separated by 3–4 mm from the Fe electrode (55). Performance curve data provided by C. Ponce de Leon

ever before. Rechargeable metal-O_2 cells are amongst the few contenders that can exceed the stored energy of the current state-of-the-art Li-ion cells. Multivalent metal-air (O_2) batteries described herein possess significant promise for high energy storage applications, but in general most examples (with the exception of primary zinc-air that has been commercialised for several years) are a long way from being a technological product. Fundamental challenges in all aspects of the cell, anode, electrolyte and cathode, need to be addressed. The major issue for aqueous based systems is the ability to recharge and cycle at high efficiency, to be resolved by the development of ever more effective bifunctional OER and ORR catalysts.

Rechargeable batteries need to be based on truly reversible reactions and the ability to cycle a cell is not proof of true reversibility. Major gaps in fundamental knowledge of all types of metal-O_2 cells remain, for example the realisation of electrolyte and materials composition that provide reversible stripping and plating of metal anodes and reversible oxide/hydroxide production and decomposition. As a result, much ground-breaking and exciting science remains to be done.

References

1. P. G. Bruce, S. A. Freunberger, L. J. Hardwick and J.-M. Tarascon, *Nature Mater.*, 2012, **11**, 19
2. G. Girishkumar, B. McCloskey, A. C. Luntz, S. Swanson and W. Wilcke, *J. Phys. Chem. Lett.*, 2010, **1**, (14), 2193
3. J.-S. Lee, S. T. Kim, R. Cao, N.-S. Choi, M. Liu, K.

T. Lee and J. Cho, *Adv. Energy Mater.*, 2011, **1**, (1), 2

4. G. L. Leclanché, 'Improvement in Combining Generating and Secondary or Accumulating Galvanic Battery', *US Patent*, 64,113; 1867
5. D. Aurbach, B. D. McCloskey, L. F. Nazar and P. G. Bruce, *Nature Energy*, 2016, **1**, (9), 16128
6. A. C. Luntz and B. D. McCloskey, *Chem. Rev.*, 2014, **114**, (23), 11721
7. X. Zhang, X.-G. Wang, Z. Xie and Z. Zhou, *Green Energy Environ.*, 2016, **1**, (1), 4
8. F. Li and J. Chen, *Adv. Energy Mater.*, 2017, **7**, (24),1602934
9. C. L. Bender, D. Schröder, R. Pinedo, P. Adelhelm and J. Janek, *Angew. Chem. Int. Ed.*, 2016, **55**, (15), 4640
10. P. Adelhelm, P. Hartmann, C. L. Bender, M. Busche, C. Eufinger and J. Janek, *Beilstein J. Nanotechnol.*, 2015, **6**, 1016
11. Y. Li, M. Gong, Y. Liang, J. Feng, J.-E. Kim, H. Wang, G. Hong, B. Zhang and H. Dai, *Nature Commun.*, 2013, **4**, 1805
12. Y. Liu, Q. Sun, W. Li, K. R. Adair, J. Li and X. Sun, *Green Energy Environ.*, 2017, **2**, (3), 246
13. T. Zhang, Z. Tao and J. Chen, *Mater. Horiz.*, 2014, **1**, (2), 196
14. T. Khoo, A. Somers, A. A. J. Torriero, D. R. MacFarlane, P. C. Howlett and M. Forsyth, *Electrochim. Acta*, 2013, **87**, 701
15. N. Wang, R. Wang, Y. Feng, W. Xiong, J. Zhang and M. Deng, *Corrosion Sci.*, 2016, **112**, 13
16. S. Yuan, H. Lu, Z. Sun, L. Fan, X. Zhu and W. Zhang, *J. Electrochem. Soc.*, 2016, **163**, (7), A1181
17. H. Xiong, K. Yu, X. Yin, Y. Dai, Y. Yan and H. Zhu, *J. Alloys Comp.*, 2017, **708**, 652
18. G. Vardar, J. G. Smith, T. Thompson, K. Inagaki, J. Naruse, H. Hiramatsu, A. E. S. Sleightholme, J. Sakamoto, D. J. Siegel and C. W. Monroe, *Chem. Mater.*, 2016, **28**, (21), 7629
19. C.-S. Li, Y. Sun, F. Gebert and S.-L. Chou, *Adv. Energy Mater.*, 2017, **7**, (24), 1700869
20. R. P. Hamlen, E. C. Jerabek, J. C. Ruzzo and E. G. Siwek, *J. Electrochem. Soc.*, 1969, **116**, (11), 1588
21. D. Aurbach, R. Skaletsky and Y. Gofer, *J. Electrochem. Soc.*, 1991, **138**, (12), 3536
22. A. Ponrouch, C. Frontera, F. Bardé and M. R. Palacín, *Nature Mater.*, 2016, **15**, 169
23. P. Reinsberg, C. J. Bondue and H. Baltruschat, *J. Phys. Chem. C*, 2016, **120**, (39), 22179
24. T. Shiga, Y. Kato and Y. Hase, *J. Mater. Chem. A*, 2017, **5**, (25), 13212
25. N. U. Pujare, K. W. Semkow and A. F. Sammells, *J. Electrochem. Soc.*, 1988, **135**, (1), 260
26. J. F. Cooper and P. K. Hosmer, 'The Behavior of the Calcium Electrode in Aqueous Electrolytes', Abstract 54, 152nd Meeting, The Electrochemical Society, Atlanta, USA, 9th–14th October, 1977, p. 25
27. Y. Zhao and T. J. VanderNoot, *Electrochim. Acta*, 1997, **42**, (11), 1639
28. M. Nestoridi, D. Pletcher, J. A. Wharton and R. J. K. Wood, *J. Power Sources*, 2009, **193**, (2), 895
29. Q. Li and N. J. Bjerrum, *J. Power Sources*, 2002, **110**, (1), 1
30. D. R. Egan, C. Ponce de León, R. J. K. Wood, R. L. Jones, K. R. Stokes and F. C. Walsh, *J. Power Sources*, 2013, **236**, 293
31. R. Mori, *RSC Adv.*, 2014, **4**, (57), 30346
32. R. Mori, *J. Electrochem. Soc.*, 2015, **162**, (3), A288
33. R. Mori, *RSC Adv.*, 2017, **7**, (11), 6389
34. M. A. Deyab, *Electrochim. Acta*, 2017, **244**, 178
35. A. R. Despić, *J. Appl. Electrochem.*, 1985, **15**, (2), 191
36. G. Cohn, D. Starosvetsky, R. Hagiwara, D. D. Macdonald and Y. Ein-Eli, *Electrochem. Commun.*, 2009, **11**, (10), 1916
37. X. Zhong, H. Zhang, Y. Liu, J. Bai, L. Liao, Y. Huang and X. Duan, *ChemSusChem*, 2012, **5**, (1), 177
38. Y. E. Durmus, Ö. Aslanbas, S. Kayser, H. Tempel, F. Hausen, L. G. J. de Haart, J. Granwehr, Y. Ein-Eli, R.-A. Eichel and H. Kungl, *Electrochim. Acta*, 2017, **225**, 215
39. A. Garamoun, M. B. Schubert and J. H. Werner, *ChemSusChem*, 2014, **7**, (12), 3272
40. D.-W. Park, S. Kim, J. D. Ocon, G. H. A. Abrenica, J. K. Lee and J. Lee, *ACS Appl. Mater. Interfaces*, 2015, **7**, (5), 3126
41. G. Cohn and Y. Ein-Eli, *J. Power Sources*, 2010, **195**, (15), 4963
42. J. Fu, Z. P. Cano, M. G. Park, A. Yu, M. Fowler and Z. Chen, *Adv. Mater.*, 2017, **29**, (7), 1604685
43. Y.-C. Lee, P.-Y. Peng, W.-S. Chang and C.-M. Huang, *J. Taiwan Inst. Chem. Eng.*, 2014, **45**, (5), 2334
44. X. Wu, G. Meng, W. Liu, T. Li, Q. Yang, X. Sun and J. Liu, *Nano Res.*, 2018, **11**, (1), 163
45. B. Li, X. Ge, F. W. T. Goh, T. S. A. Hor, D. Geng, G. Du, Z. Liu, J. Zhang, X. Liu and Y. Zong, *Nanoscale*, 2015, **7**, (5), 1830
46. H.-F. Wang, C. Tang, B. Wang, B.-Q. Li and Q. Zhang, *Adv. Mater.*, 2017, **29**, (35), 1702327
47. B. Chen, X. He, F. Yin, H. Wang, D.-J. Liu, R. Shi, J. Chen and H. Yin, *Adv. Funct. Mater.*, 2017, **27**, (37), 1700795

48. Z. Cui, Y. Li, G. Fu, X. Li and J. B. Goodenough, *Adv. Mater.*, 2017, **29**, (40), 1702385
49. Z. Cui, G. Fu, Y. Li and J. B. Goodenough, *Angew. Chem. Int. Ed.*, 2017, **56**, (33), 9901
50. J. Fu, F. M. Hassan, C. Zhong, J. Lu, H. Liu, A. Yu and Z. Chen, *Adv. Mater.*, 2017, **29**, (35), 1702526
51. W. Niu, Z. Li, K. Marcus, L. Zhou, Y. Li, R. Ye, K. Liang and Y. Yang, *Adv. Energy Mater.*, 2018, **8**, (1), 1701642
52. Y.-T. Lu, Y.-J. Chien, C.-F. Liu, T.-H. You and C.-C. Hu, *J. Mater. Chem. A*, 2017, **5**, (39), 21016
53. K. Vijayamohanan, T. S. Balasubramanian and A. K. Shukla, *J. Power Sources*, 1991, **34**, (3), 269
54. L. Öjefors and L. Carlsson, *J. Power Sources*, 1978, **2**, (3), 287
55. H. Cnobloch, Proceedings of the 88th Convention of the Battery Council International Future Clean Silent Power, Mexico City, Mexico, 25th–29th April, 1976, pp. 39–48
56. A. Inoishi, S. Ida, S. Uratani, T. Okano and T. Ishihara, *RSC Adv*., 2013, **3**, (9), 3024
57. X. Zhao, N. Xu, X. Li, Y. Gong and K. Huang, *RSC Adv*., 2012, **2**, (27), 10163
58. R. D. McKerracher, C. Alegre, V. Baglio, A. S. Aricò, C. Ponce de León, F. Mornaghini, M. Rodlert and F. C. Walsh, *Electrochim. Acta*, 2015, **174**, 508
59. H. A. Figueredo-Rodríguez, R. D. McKerracher, M. Insausti, A. G. Luis, C. Ponce de León, C. Alegre, V. Baglio, A. S. Aricò and F. C. Walsh, *J. Electrochem. Soc.,* 2017, **164**, (6), A1148

The Authors

Laurence Hardwick is Professor of Electrochemistry and Director of the Stephenson Institute for Renewable Energy within the Department of Chemistry at the University of Liverpool, UK. His research interests focus on understanding reaction mechanisms of metal-air batteries and the development of surface sensitive *in situ* electrochemical Raman and infrared spectroscopies to probe battery electrode-electrolyte interfaces.

Carlos Ponce de León Albarrán is Senior Lecturer, Energy Technology Group within Engineering and the Environment at the University of Southampton, UK. He is working from an electrochemical engineering perspective in aqueous metal-air batteries, water treatment, metal ion removal, characterisation of novel electrode materials, electrochemical strategies for pollution control and redox flow cells for energy conversion.